Acta Crystallographica Section C
Crystal Structure Communications
ISSN 0108-2701

Room-temperature monoclinic and low-temperature triclinic phase-transition structures of *meso*-octamethylcalix[4]pyrrole–dimethyl sulfoxide (1/1)

Vincent M. Lynch,[a]* Philip A. Gale,[b] Jonathan L. Sessler[a] and David Madeiros[a]

[a]Department of Chemistry and Biochemistry, University of Texas at Austin, Austin, TX 78712, USA, and [b]Department of Chemistry, University of Southampton, Southampton SO17 1BJ, England
Correspondence e-mail: vmlynch@mail.utexas.edu

Received 17 April 2001
Accepted 27 September 2001

Crystals of the title complex, $C_{28}H_{36}N_4{\cdot}C_2H_6OS$, undergo a phase transition between room temperature and 198 K, as determined by X-ray diffraction techniques. A monoclinic form is observed at room temperature, while a triclinic modification is found at 198 K, with Z' changing from 1 to 2. Differential scanning calorimetry (DSC) of the calixpyrrole–dimethyl sulfoxide complex revealed a series of phase changes between 273 and 243 K. The transition from the room-temperature monoclinic form to the low-temperature triclinic form is reversible, as determined by changes in the cell dimensions from remeasuring selected reflections at room temperature and at temperatures below 223 K. The uncomplexed calix[4]pyrrole molecule shows no phase changes occurring between room temperature and 233 K, the low-temperature limit of the DSC.

Comment

We have shown that calix[4]pyrroles are capable of binding anions (Gale *et al.*, 1996, 1997; Sessler *et al.*, 1996) and neutral guest species (Allen *et al.*, 1996) in both solution and the solid state. Anion complexes of calix[4]pyrroles have been found to adopt solely the cone conformation in the solid state, whereas neutral guest complexes adopt a range of conformations [*e.g.* 1,3-alternate (methanol) and 1,2-alternate (dimethylformamide)]. The structure of the dimethyl sulfoxide (DMSO) complex, (I), of *meso*-octamethylcalix[4]pyrrole is presented herein. The crystals were found to undergo a phase change between 273 and 243 K using differential scanning calorimetry (DSC). The DSC results are not completely reversible, which may be due to solvent loss during the warming cycle of the scans.

The structure reveals that the calix[4]pyrrole molecule exists in the 1,3-alternate conformation in both the low-temperature triclinic form and the room-temperature monoclinic form. The triclinic form is reported in a non-standard pseudo-monoclinic setting for ease of comparison with the monoclinic form. The triclinic form has two molecules per

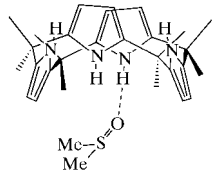

(I)

asymmetric unit. Atoms of molecule 1 are related to the equivalent atoms of molecule 2 (marked by a prime) by a pseudo-glide plane given by $x, \frac{1}{2}-y, -\frac{1}{2}+z$. There is no change in the conformation of the calix[4]pyrrole macrocycle or in the macrocycle-to-solvent interaction upon cooling. The DMSO O atom is hydrogen bonded to a single pyrrole group of the calix[4]pyrrole molecule. In the monoclinic phase, the geometry of the N1—H1N···O1*A* hydrogen-bonding interaction is N···O = 2.982 (4) Å, H···O = 1.99 (4) Å and N—H···O = 169 (3)°. In the triclinic phase, there are two independent hydrogen-bonding interactions, *i.e.* N1—H1N···O1*A* [N···O = 2.985 (5) Å, H···O = 2.10 (5) Å and N—H···O = 177 (5)°] and N1′—H1′N···O1*A*′ [N···O = 2.961 (5) Å, H···O = 2.03 (5) Å and N—H···O = 175 (5)°].

The calix[4]pyrrole–DMSO complex forms columns parallel to the *c* axis. Within a column, long-range N—H···O interactions between a pyrrole group in one complex and the DMSO O atom of an adjacent complex are observed. In the monoclinic phase, the columns are composed of molecules related by the *c*-glide plane operation. The N···O contact is 3.617 (5) Å between O1*A* and N3 related by $x, \frac{1}{2}-y, -\frac{1}{2}+z$, while the H3N···O1*A* contact is 2.74 (4) Å and the N—H···O

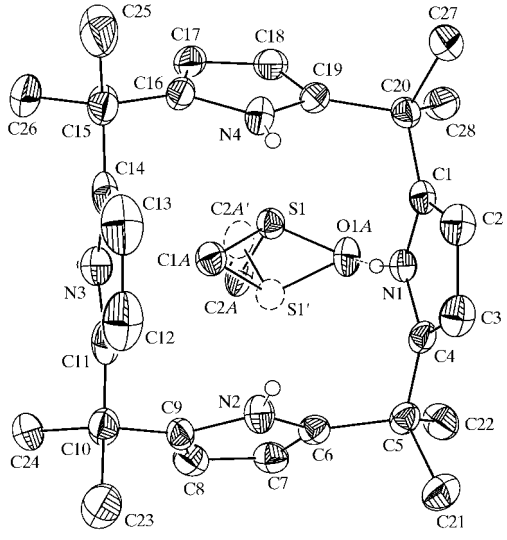

Figure 1
View showing the atom-labeling scheme for the room-temperature phase of the *meso*-octamethylcalix[4]pyrrole–DMSO complex. Ellipsoids are scaled to the 30% probability level. Most H atoms have been removed for clarity. Dashed ellipses represent the lower occupancy atoms [35 (1)%] of the disordered DMSO molecule.

angle is 158 (3)°. In the triclinic phase, the columns are composed of molecules related by a *c*-axis translation. There are two unique long-range N—H···O contacts in the triclinic phase. The geometry of the first contact is O1*A*···N3′ = 3.558 (6) Å, O1*A*···H3′N = 2.75 (5) Å and N—H···O = 156 (4)°. The geometry of the second contact is O1*A*′···N3(*x*, *y*, *z* − 1) = 3.554 (6) Å, H3N···O1*A* = 2.63 (5) Å and N—H···O = 164 (4)° (Fig. 2).

These long-range N—H···O contacts act to stabilize complex-to-complex interactions within a column. As a result, there is little difference in structure observed between the monoclinic and triclinic phases along a column. For example, if the atoms of the calix[4]pyrrole of molecule 1 of the triclinic phase are superimposed onto the equivalent atoms of the monoclinic phase, the *c*-glide symmetry relative of the monoclinic phase is nearly superimposed on top of molecule 2 of the triclinic phase. The average distance between equivalent atoms of these latter two molecules is less than 0.12 Å.

The loss of symmetry on cooling results from a change in the column-to-column packing. The change is illustrated in Fig. 3. Whereas the atom shift within a column was found to be small, the shift between columns is substantial. To determine the change in position with reference to the monoclinic cell, a second molecule of the calix[4]pyrrole–DMSO complex for the monoclinic phase was generated by $1 - x, \frac{1}{2} + y, \frac{3}{2} - z$. For the triclinic phase, molecule 2 was moved to a position that would most closely correspond to the twofold screw axis relative in the monoclinic cell. This was accomplished by inverting molecule 2 though the crystallographic inversion center at $\frac{1}{2},\frac{1}{2},\frac{1}{2}$. Using the utility *OFIT* in *SHELXTL/PC* (Sheldrick, 1998), molecule 1 of the triclinic phase was superimposed onto the calix[4]pyrrole molecule in the monoclinic phase. Molecule 2, related by $1 - x, 1 - y, 1 - z$, lies near the twofold screw axis relative of the monoclinic phase. The average distance between the equivalent atoms of these latter two molecules is 0.78 Å.

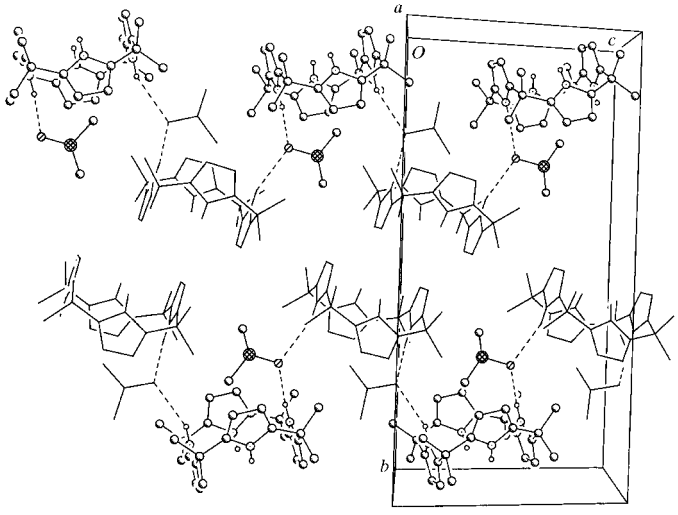

Figure 2
Unit-cell packing diagram for the low-temperature triclinic phase showing portions of two hydrogen-bonded columns extending parallel to the *c* axis. Within one column, molecules represented in wireframe form are related by the approximate *c*-glide to the molecules shown in ball-and-stick form. Dashed lines are indicative of N—H···O hydrogen-bonding interactions.

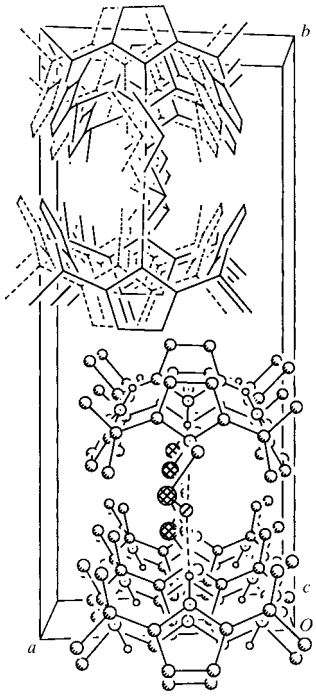

Figure 3
Fit by least squares of the atoms of molecule 1 of the low-temperature phase to the equivalent atoms of the room-temperature phase. All non-H atoms of the calix[4]pyrrole molecule were included in the fit. The columns of the monoclinic phase are shown in ball-and-stick and in wireframe form. The offset of the triclinic form, which is displayed as dashed lines, results primarily from a shift along the *a* axis.

Experimental

Details of the synthetic procedures have been published elsewhere (Gale *et al.*, 1996). Crystals were grown by slow evaporation from a DMSO solution.

Monoclinic (I)

Crystal data

$C_{28}H_{36}N_4{\cdot}C_2H_6OS$
M_r = 506.74
Monoclinic, $P2_1/c$
a = 10.411 (2) Å
b = 23.586 (6) Å
c = 12.482 (3) Å
β = 107.71 (2)°
V = 2919.7 (12) Å^3
Z = 4
D_x = 1.153 Mg m^{-3}
Mo $K\alpha$ radiation
Cell parameters from 40 reflections
θ = 8.8–10.9°
μ = 0.14 mm^{-1}
T = 298 (2) K
Trapezoidal prism, colorless
0.34 × 0.34 × 0.24 mm

Data collection

Siemens *P*3 diffractometer
ω scans
6290 measured reflections
5109 independent reflections
2069 reflections with $I > 2\sigma(I)$
R_{int} = 0.047
θ_{max} = 25.0°
$h = -1 \rightarrow 12$
$k = -1 \rightarrow 28$
$l = -14 \rightarrow 14$
4 standard reflections every 96 reflections
intensity decay: <2%

Refinement

Refinement on F^2
$R[F^2 > 2\sigma(F^2)] = 0.071$
$wR(F^2) = 0.152$
$S = 0.97$
5109 reflections
359 parameters
H atoms treated by a mixture of independent and constrained refinement
$w = 1/[\sigma^2(F_o^2) + (0.0482P)^2]$ where $P = (F_o^2 + 2F_c^2)/3$
$(\Delta/\sigma)_{max} = 0.016$
$\Delta\rho_{max} = 0.16$ e Å^{-3}
$\Delta\rho_{min} = -0.17$ e Å^{-3}

Triclinic (I)

Crystal data

$C_{28}H_{36}N_4{\cdot}C_2H_6OS$
$M_r = 506.74$
Triclinic, $P\overline{1}$
$a = 10.362$ (3) Å
$b = 23.468$ (10) Å
$c = 12.373$ (7) Å
$\alpha = 90.23$ (4)°
$\beta = 107.64$ (4)°
$\gamma = 88.35$ (3)°
$V = 2866$ (2) Å^3
$Z = 4$
$D_x = 1.174$ Mg m^{-3}
Mo $K\alpha$ radiation
Cell parameters from 27 reflections
$\theta = 8.5$–11°
$\mu = 0.14$ mm^{-1}
$T = 198$ (2) K
Prism, colorless
0.34 × 0.34 × 0.26 mm

Data collection

Siemens *P*4 diffractometer
ω scans
11 862 measured reflections
10 061 independent reflections
5213 reflections with $I > 2\sigma(I)$
$R_{int} = 0.042$
$\theta_{max} = 25.0°$
$h = -5 \rightarrow 12$
$k = -27 \rightarrow 27$
$l = -14 \rightarrow 14$
4 standard reflections
every 96 reflections
intensity decay: <2%

Refinement

Refinement on F^2
$R[F^2 > 2\sigma(F^2)] = 0.081$
$wR(F^2) = 0.155$
$S = 1.11$
10 046 reflections
718 parameters
H atoms treated by a mixture of independent and constrained refinement
$w = 1/[\sigma^2(F_o^2) + (0.0536P)^2 + 6.1009P]$ where $P = (F_o^2 + 2F_c^2)/3$
$(\Delta/\sigma)_{max} = -0.028$
$\Delta\rho_{max} = 0.40$ e Å^{-3}
$\Delta\rho_{min} = -0.27$ e Å^{-3}
Extinction correction: *SHELXTL*/*PC*
Extinction coefficient: 0.0015 (4)

The crystals cracked when quickly immersed in a cold nitrogen gas stream at 198 K. However, the crystals generally remained intact when cooled slowly to 198 K although, at this temperature, the diffraction peaks were quite broad. The low-temperature cell had nearly monoclinic metric symmetry. Because of this and the fact that the crystals cracked upon quick cooling, we investigated the room-temperature structure as well. Crystals of the DMSO–calix[4]pyrrole complex decompose slowly at room temperature. The room-temperature data set was accomplished by mounting a crystal in a capillary containing a small amount of the mother liquor. The ends of the capillary were sealed with epoxy. A different crystal was used for the low-temperature data set. In both crystals, the DMSO molecule was found to be disordered in such a way that the S atom appears in two positions, above and below the plane through the remaining atoms of the DMSO molecule. The site-occupancy factors were initially determined by refining the S-atom site-occupancy factors to sum to 1 with a common U_{iso} value. In the final stages of refinement, two positions for one of the methyl C atoms could be resolved and both the S- and C-atom occupancies were refined. Interestingly, the site occupancies of the major and minor forms refined to different values for the two different crystals. The H atoms on N atoms were observed from a difference map and refined with isotropic displacement parameters [the N—H range was 0.83 (4)–1.01 (4) Å for the monoclinic form and 0.83 (5)–0.94 (5) Å for the triclinic form]. The remaining H atoms were calculated in idealized positions (C—H = 0.96 Å). For the room-temperature structure, the regions around the methyl C atoms of the DMSO molecule where H atoms would be expected to be located showed the highest residual electron density. At this point, idealized H-atom positions with site-occupancy factors weighted to account for the disordered DMSO molecule were included in the model. The refinement of the triclinic phase proceeded normally. There were no unusual correlation coefficients between parameters of atoms related by the pseudo-glide plane. High correlation coefficients were observed between parameters of atoms of the disordered DMSO molecules for both phases.

For both compounds, data collection: *XSCANS* (Siemens, 1994); cell refinement: *XSCANS*; data reduction: *XSCANS*; program(s) used to solve structure: *XS* in *SHELXTL*/*PC* (Sheldrick, 1998); program(s) used to refine structure: *XL* in *SHELXTL*/*PC*; molecular graphics: *XP* in *SHELXTL*/*PC*.

Funding for this work was provided by the Robert A. Welch Foundation and the National Institutes of Health. PAG thanks the Fulbright Commission for a postdoctoral fellowship.

Supplementary data for this paper are available from the IUCr electronic archives (Reference: FR1336). Services for accessing these data are described at the back of the journal.

References

Allen, W. E., Gale, P. A., Brown, C. T., Lynch, V. M. & Sessler, J. L. (1996). *J. Am. Chem. Soc.* **118**, 12471–12472.
Gale, P. A., Sessler, J. L., Allen, W. E., Tvermoes, N. A. & Lynch, V. (1997). *Chem. Commun.* pp. 665–666.
Gale, P. A., Sessler, J. L., Kral, V. & Lynch, V. (1996). *J. Am. Chem. Soc.* **118**, 5140–5141.
Sessler, J. L., Andrievsky, A., Gale, P. A. & Lynch, V. (1996). *Angew. Chem. Int. Ed. Engl.* **35**, 2782–2785.
Sheldrick, G. M. (1998). *SHELXTL*/*PC*. Release 5.1. Bruker AXS Inc., Madison, Wisconsin, USA.
Siemens (1994). *XSCANS*. Version 2.10b. Siemens Analytical X-ray Instruments Inc., Madison, Wisconsin, USA.